Full length article

Zinc dialkyldithiophosphates adsorption and dissociation on ferrous substrates: An *ab initio* study

Francesca Benini, Paolo Restuccia, M. Clelia Righi *

Department of Physics and Astronomy, University of Bologna, Viale Carlo Berti Pichat 6/2, Bologna, 40127, Italy

ARTICLE INFO

ABSTRACT

Zinc dialkyldithiophosphates (ZDDPs) have been commonly used as anti-wear additives in the automotive industry for the past 80 years. Despite their widespread use, a general agreement on their primary functioning mechanism is still lacking. The morphology and composition of the ZDDPs phosphate-based tribofilm, which is essential for its lubricant functioning, have been widely studied experimentally. However, the formation process and the relevant driving forces are still largely debated. In particular, it is unclear whether the stress-induced molecular dissociation occurs in the bulk oil or on the substrate. In this work, we employ *ab initio* density-functional theory simulations to compare ZDDP fragmentation in vacuum and over a reactive substrate, considering the effects of surface oxidation on the dissociation path. To do so, we developed a computational protocol to study the effects of shear stress on molecules. Our results show that the molecular dissociation is endothermic in the absence of a supporting substrate, while in the presence of an iron substrate, it becomes highly energetically favoured. Moreover, the presence of the substrate changes the reaction path, inducing the detachment of organophosphorus units from Zn-S ones. At the same time, surface oxidation reduces the molecule–substrate interaction. These findings provide valuable insights into the early stages of the formation of phosphate-based tribofilms.

1. Introduction

After more than 80 years since their discovery, zinc dialkyldithio-phosphates (ZDDPs) are still the most used anti-wear additives in the automotive industry [1–3]. Indeed, this class of materials is known for their capability to prevent wear, especially on steel [4–6], thanks to the formation of a glassy phosphate-based tribofilm [1,7].

Many details on the ZDDP tribofilm chemical composition and morphology are known thanks to the great effort that has been put experimentally into its characterization [7–14]. The film, typically around 80–150 nm thick and composed of flat-topped pads [10], consists of a superficial layer of zinc and iron polyphosphate and/or phosphate; closer to the steel surface it presents a sulfur-rich layer [1,8,13]; finally, although believed amorphous for years, it was recently found that ZDDP tribofilms hide a nanocrystalline structure, promoted by prolonged rubbing, which improves their durability [11].

Concerning the tribofilm formation process, the following main steps have been proposed [11,14]: first, surface adsorption and the initial formation of iron disulphide take place; secondly, the alkyl groups of the ZDDP molecule transfer from oxygen to sulfur, converting dialkylthiophosphate to dithionyl phosphate; thirdly, intermolecular reactions enable phosphates to polymerize to build polyphosphate

chains, the building blocks for the tribofilm; and finally, the amorphous film forms, which then becomes crystalline within a depolymerization process enhanced by prolonged rubbing at elevated temperatures [11].

However, despite such general consensus, there are still matters of debate, for instance, concerning what specifically drives ZDDP dissociation and the subsequent film formation, as well as the exact fragmentation path followed by the molecule and the role played by the substrate in such process [12,13,15]. Concerning the latter, some authors proposed that the substrate hardness might affect tribofilm quality [4,16,17]. Indeed, the appearance of a protective film in tribo-logical conditions is a common phenomenon, and many factors might affect its formation. This is why a deep understanding of the different roles played by various physical quantities, such as compressive and shear stress, temperature, and the interaction with the substrate, is crucial to design new lubricant additives [18] and unveil the functionality of commercial ones [19]. These contributions are difficult to isolate experimentally in actual tribological conditions since they are all at play simultaneously at the nano-asperity contact.

Among all of these quantities, it has been suggested that shear stress within the base oil might be the driving force for ZDDP tribofilm formation. This hypothesis, described through the Stress-Promoted Thermal

---

Activation model [7,8,12,20], has been strengthened by experimental evidence of ZDDP tribofilm formation on a variety of substrates, ranging from metals [21,22] to ceramics [23–25], DLC coatings [26] and silicon [4], suggesting that the molecule–substrate chemical interaction plays a minor role in the phenomenon. However, recent studies emphasized the role of reactive substrates, like the ones exposed during tribological experiments, as the primary driving force in the dissociation and tribofilm formation of commercial lubricant additives [18,27,28]. More in general, the importance of surface reactivity has been highlighted in different research field through the years, like in catalysis [29,30].

Finally, despite the widespread use of ZDDP additives, there is a scarcity of theoretical atomistic simulations that can provide insights into the ZDDP tribofilm formation process. In particular, the fundamental steps of the chemical reaction paths leading to the ZDDP dissociation, inaccessible from experiments, and the possible role of the molecule–substrate interaction are still missing. Indeed, none of the limited numbers of computational works concerning ZDDP takes into account the presence of a substrate [15,31–34]. In this work, we employ density-functional theory (DFT) to investigate ZDDP fragmentation on iron, oxygen-passivated and oxidized iron substrates relevant to many technological applications. We study the dissociation path followed by the ZDDP molecule when bonds are stretched in vacuum to model the situation in which stresses arise in chemically non-reactive base oils and compare it with molecule fragmentation on ferrous substrates. In this way, we identified the most favourable dissociation path and analyzed the effect of substrate oxidation on ZDDP adsorption.

2. Methods

All calculations were performed using spin-polarized Density Functional Theory (DFT) as implemented in version 6.8 of the Quantum Espresso suite [35–37] except those concerning hematite, for which the version 7.2 was employed. The exchange–correlation functional was described using the generalized gradient approximation (GGA) within the Perdew–Burke–Ernzerhof (PBE) parametrization [38]. Two different computational setup have been employed for the (001) hematite surface description and the other calculations. For the former, we exploited DFT+ U [39] with a choice for the Hubbard parameter of 4.2 eV, as found in other works concerning adsorption on hematite [40,41] and specifically suited for the Vanderbilt ultrasoft pseudopotentials used. The kinetic energy cutoff for the wave functions was set to 50 Ry, with a cutoff for charge densities of 400 Ry. We assigned the spin of d electrons localized on Fe atoms to describe the antiferromagnetic character of this material [42]. A gaussian smearing with a 0.02 Ry width was also included.

Concerning all the other calculations, the kinetic energy cutoff for the wave functions was set to 40 Ry, with a cutoff for charge densities of 320 Ry. A gaussian smearing with a 0.001 Ry width was included to describe occupations around the Fermi level better. The electronic configuration of atoms was described using ultrasoft pseudopotentials in the RRKJ parametrization [43].

The default energy and forces convergence threshold criteria (i.e., 10^{-4} Ry and 10^{-3} Ry/Bohr, respectively) were used in all calculations to optimize the structural geometries. The geometrical configuration and computational setup we used to describe the ZDDP molecule were already tested by our group in a previous work [44]. In particular, the two lateral alkyl chains have been reduced to methyl groups to minimize the computational cost. Here we study the interaction of the ZDDP molecule with five different substrates: a clean Fe(110) four-layers thick slab, a four-layer thick (001) hematite slab (Fig. 3a) and, by passivating the clean Fe slab with oxygen atoms on both sides, oxidized Fe slabs with 0.25 ML (Fig. 1a), 0.5 ML (Fig. 1b) and 1 ML (Fig. 1c) O-coverages, respectively.

We studied the ZDDP fragmentation by bond stretching [45] comparing the results obtained in vacuum and with the presence of the clean Fe substrate. Thanks to this approach, we can accurately describe the most effective dissociative path and the role played by the substrate. We placed the molecule vertically in a large supercell to carry out this task in a vacuum. We then performed a sequence of relax calculations keeping the central Zn atom fixed while displacing firstly a P, then O, and finally a C atom of 0.2 Å respectively along the z direction at each step, reaching a total displacement of 5 Å. The z coordinates of the displaced atoms were kept fixed, and the optimized coordinates of each step were used as the initial configuration for the next step. An analogous procedure was performed for the case of the molecule on the iron slab. We considered the optimized molecule adsorbed over the substrate as a starting configuration. Then, we stretched the molecule by displacing first P, then O and finally a C atom along the direction parallel to the surface, namely the x direction, keeping their x coordinate fixed together with the in-plane coordinates of the Zn atom. In this case, we reached a total displacement of 3 Å, which was enough to see the complete fragmentation of the molecule. We could then compute the reaction energies and force components acting on the fixed atoms at each step along the z (x) direction for the stretching in the vacuum (Fe substrate) case. We expressed the obtained forces as pressures dividing them by the in-plane area of the cell employed for the molecule in vacuum (2.76 nm^2) to allow for a rough estimation of the shear stress that should be applied to obtain the corresponding molecular deformation. This bond-stretching procedure can provide an estimate of the dissociation pathway in the presence of mechanical stresses applied.

To study the adsorption on surfaces, we employed large 6 × 4 orthorhombic supercells containing 48 atoms per layer for iron and O-passivated iron slabs to accommodate a ZDDP molecule preventing the interaction among replicas. Moreover, a reasonable amount of void (at least 10 Å) was added to each cell to guarantee a sufficient vertical distance between system replicas. The resulting supercell dimensions were 17.10 Å × 16.12 Å × 30.78 Å. The latter was obtained after optimizing a smaller 2 × 2 cell. Concerning adsorption on hematite, due to the high computational cost of the system, smaller 3 × 2 orthorhombic supercells were used. Considering the large dimensions of the supercell, we used a Γ point sampling of the Brillouin zone. We computed adsorption energies as follows:

$$E_{ads} = E_{tot} - (E_{surf} + E_{adsorbate}) \qquad (1)$$

where E_{tot} is the energy of the optimized system composed of the substrate and the adsorbed molecule/atom, while E_{surf} ($E_{adsorbate}$) is the energy of the isolated surface (adsorbate).

We used the molecular fragments identified by the bond stretching study to study the ZDDP dissociation over iron substrates. In particular, we employed Xsorb [46], a Python-based code designed by our group, to identify the optimal site and configuration for molecular adsorption. Starting from the optimized molecule and surface, the software automatically tests different molecular orientations and symmetry sites on the surface performing a preliminary screening through partial structural optimizations based on density functional theory, until the ideal configuration is found and fully optimized. Finally, the dissociation energy E_{frag} is computed as follows:

$$E_{frag} = \sum_{n=1}^{N} E_{F_n} - (N \times E_{surf} + E_{mol}) \qquad (2)$$

where E_{F_n} represents the total energy of the most stable systems composed of the surface and each fragment alone at a time, and E_{surf} (E_{mol}) represents the energy of the isolated surface (molecule). The value of N in the formula depends on how many molecular fragments were generated. In our case, $N = 2$, 3 and 4, respectively.

We further studied the ZDDP dissociative path looking at what happens at the interface of two Fe (or 0.25 ML and 1 ML oxidized Fe) surfaces in the presence of 1 GPa external load. To achieve this task, we realized uniaxial compressions in which we reduced the vertical
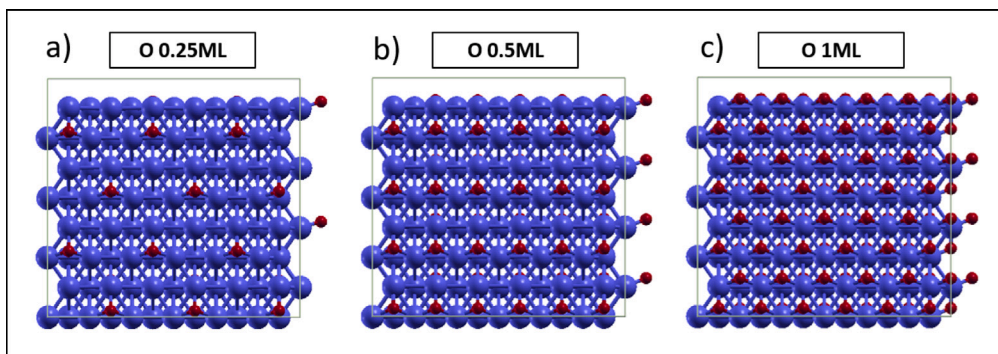
Fig. 1. The oxidized substrates modelled in this study: 0.25 ML (panel a), 0.5 ML (panel b) and 1 ML O-passivated Fe (panel c). From now on, Fe will be represented in blue and O in red.
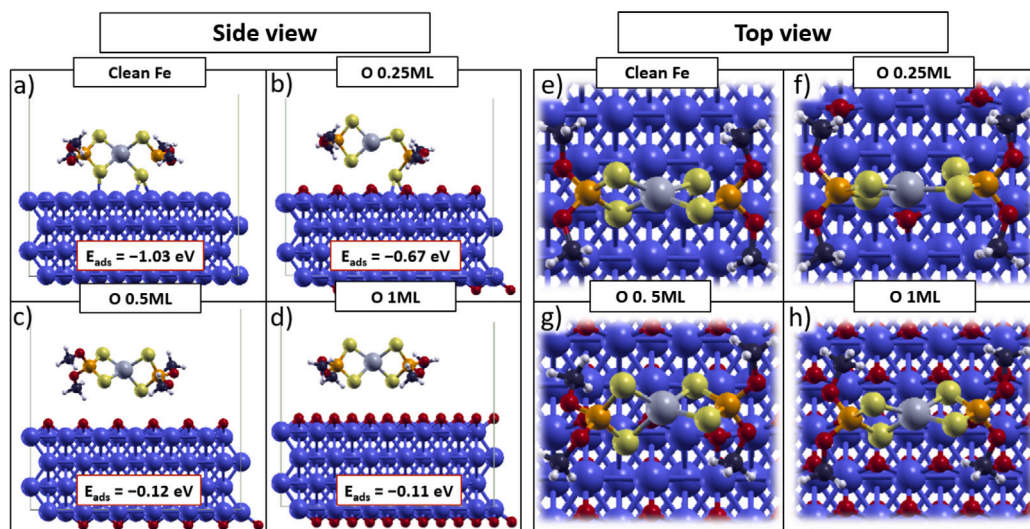

Fig. 2. Side (left) and top (right) view of ZDDP adsorption on (a), (e) clean Fe and O passivated Fe with three different O coverages: (b), (f) 0.25 ML, (c), (g) 0.5 ML and (d), (h) 1 ML respectively. Adsorption energies are also reported. From now on, P, Zn, C, H and S atoms are represented in orange, grey, black, white and yellow, respectively.

size of the cell and allowed the ZDDP molecule to interact with one side of the slab and its own replica to simulate the interface. This approach induced molecular dissociation and gave us insights into the bond breaking that takes place at the interface under load.

3. Results and discussion

Here we report the results of our simulations: first, we analyse the effect of iron oxidation on the adsorption of molecular ZDDP. Secondly, we compare ZDDP dissociation in vacuum and with a clean substrate. In a previous work [47] we studied the interaction of the lubricant additive, in that case MoDTC, with 1-hexene, a simple approximation of a non-polar solvent commonly present in base oils. We found the interaction energies for these systems are in the order of meV, significantly lower than those found for the adsorption of the additives on reactive ferrous substrates. Moreover, from a configurational point of view, the interaction resulted only in a bending of the molecules due to the mild attraction of the terminal methyl groups to the alkenes without any chemical dissociation. Other atomic species, such as sulphur, did not participate in the interaction. ZDDP is expected to interact similarly with base oil, making our atom-pulling procedure in vacuum representative of non-chemically reactive interaction. We then look at the effect of substrate oxidation on the dissociation energies and finally consider how the dissociation proceeds when the molecule is set at the interface between two facing substrates.

3.1. ZDDP adsorption

The first important step in forming ZDDP tribofilms is the adsorption of the molecules on the substrate [1,8,14]. Modelling bulk Fe oxides, like hematite, is extremely computationally demanding and requires an exquisite fine-tuning of the computational parameters. Thus, we modelled the effect of iron oxidation using iron slabs passivated by oxygen atoms, as done in previous studies [19,27,44]. In addition to the clean iron substrate, we simulated three different degrees of surface O-passivation, namely 0.25 ML, 0.5 ML and 1 ML, shown in Fig. 1. We compared these results with those obtained by modelling the interaction of ZDDP with a anti-ferromagnetic hematite (001) surface, portrayed in Fig. 3, in order to test the accuracy of our approximation and the possible effects of magnetization on adsorption.

After fully optimizing the geometry of the adsorbed molecule/substrate system, E_{ads} was computed following Eq. (1). The optimized configurations and corresponding adsorption energies, are reported in Fig. 2. The adsorption energies are negative for all the considered systems, indicating that molecular adsorption is energetically favourable. This is in agreement with the experimental evidence that ZDDP undergoes chemisorption and thermal decomposition [1,48]. However, oxygen passivation significantly reduces the interaction of the ZDDP molecule with Fe. In particular, E_{ads} decreases by about one order of magnitude, from −1.03 eV for the bare iron substrate to −0.12 and −0.11 eV for the half and fully passivated substrates. The 0.25 ML passivated substrate maintains a mild reactivity, with $E_{ads} = -0.67$ eV, as the ZDDP undergoes structural deformations leading to bonds
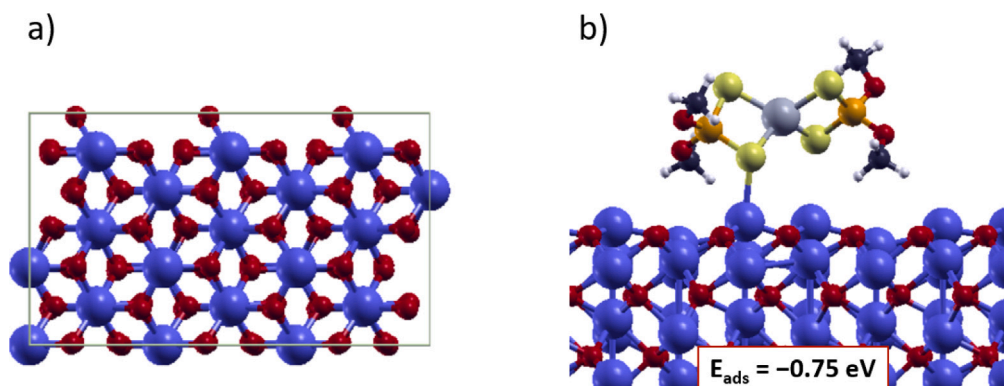
Fig. 3. (a) Top view of the 3 × 2 supercell for the hematite (001) surface employed and side view of ZDDP adsorption on it (b). The adsorption energy value obtained is reported in panel (b).
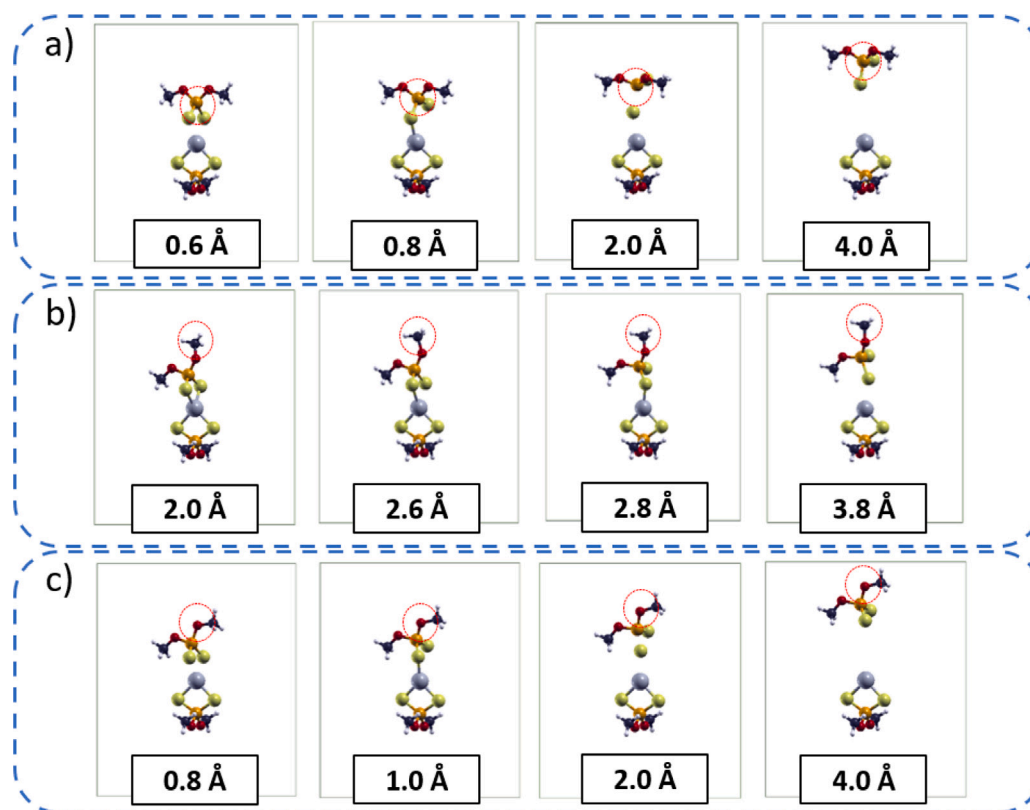

Fig. 4. Configurations resulting from pulling, respectively, a P atom (panel a), a C atom (panel b) and an O atom (panel c). The atom pulled is highlighted with a dotted red circle and the displacement along *z* is reported.

breaking and S interaction with iron atoms (Fig. 2b). The adsorption over this substrate is the closest energetically to hematite, where E_{ads} is −0.75 eV. Therefore, we can use the 0.25 ML O-passivated substrate as a reference model for the energetics of ZDDP on hematite. It is also interesting to note that both systems have similar adsorption energies despite having opposite magnetic properties, suggesting that magnetization should play a minor role in the energetics of ZDDP adsorption.

We can also compare these ZDDP adsorption data with the ones we obtained on simple metal and light alloys [44]. It is worth noting that those adsorption energies, ranging from −0.05 eV for Mg(0001) to −0.15 eV for Al(331), are around one order of magnitude higher than those on clean iron and hematite and are comparable only with high levels of oxygen passivation. This result could hint at why ZDDP and other standard oil additives do not provide the same anti-wear and friction reduction efficiency when employed on lightweight alloys [49].

3.2. Shear-induced dissociation of ZDDP in the absence and in the presence of a substrate

The geometry configurations along the stretching bond procedure are shown in Fig. 4. Confirming what we previously obtained in Ref. [44], we find that, whatever atom is pulled, the most favourable fragmentation pattern involves breaking the Zn-S bonds. Therefore, we found that in vacuum or inside the lubricating oil, when shear stress is applied to the molecule, the Zn-S bonds are the less energetically demanding to break, as also reported in the literature [7,50].

In panel (a) of Fig. 5, the energy variation as a function of the atom displacement along the *z* direction is displayed for all three pulling atoms, whereas in panel (b) the forces per unit area acting on P, C and O are shown. In all three cases, the energy increases during the atom pulling until a plateau is reached at a fragment distance where the interaction is negligible. Independently from the pulling atom, the
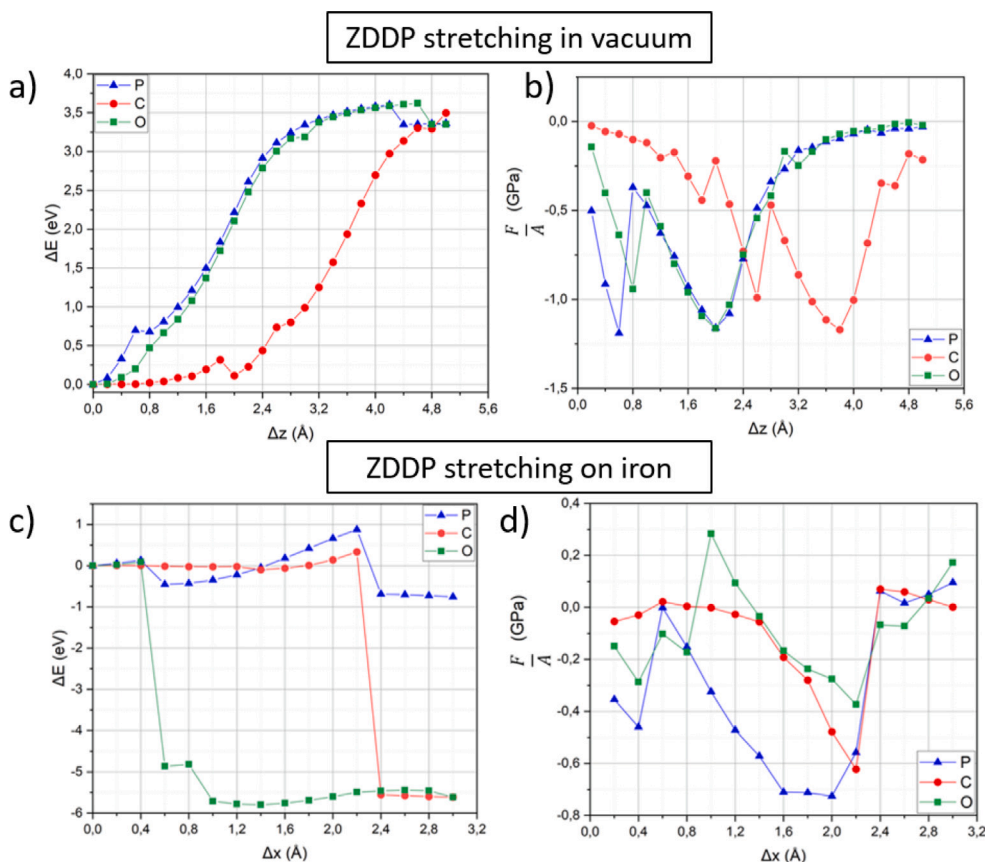
ZDDP stretching in vacuum

ZDDP stretching on iron

Fig. 5. Energy variation as a function of atom displacement along the *z* (*x*) direction in panel a (c) alongside force per unit area on P, C and O in panel b (d) for the ZDDP molecule stretching in vacuum (on iron substrate). *F* is the value of the force acting on P, C and O whereas *A* is the in-plane area of the cell. A positive (negative) value of *F* indicates a force with the same (opposite) direction of the *z* (*x*) axis in the reference system.

detachment of the $S_2P(OCH_3)_2$ fragment has an associated energy cost of about 3.5 eV. Alongside the energy, the force divided by the in-plane cell area acting on the pulled atoms provides a consistent picture with a maximum increase of the resistant forces per unit area when bond breaking occurs of about 1.2 GPa.

The results of the bond-stretching procedure on the iron substrate are summarized in Fig. 5c and d. Interestingly, the energy and the resistant stress in the presence of a substrate are much lower than those in the absence, indicating that the presence of the substrate makes the molecular dissociation much easier than in the oil. Indeed, the dissociated fragments are stabilized by the substrate, as visible from the reaction energies that diminished significantly to around −6 eV for both C and O pulling (Fig. 5c). In the case of P, the reaction energy is significantly larger due to the shallower interaction of the Zn-S central unit compared to the other two cases (as shown in Fig. 6a).

Not only the energies and forces are dramatically changed by the presence of the substrate, but also the dissociation path is different. As shown in Fig. 6, the most favourable dissociation path involves breaking the P-S bonds. We calculated the energy cost/gain for this fragmentation on the substrate considering both the clean and oxygen-terminated (1 ML coverage) iron surface (Fig. 7a). Further dissociation steps were also considered for the clean surface (Fig. 7b, c), which show that the $P(OCH_3)_2$ groups are released and chemisorbed to the iron substrate, leaving the central Zn-S units and isolated S atoms adsorbed on iron, with high energy gain. These results agree with the experimental observation of an S-rich iron layer and phosphate layers within the tribofilm.

Our results suggest that the substrate-mediated dissociation is much more probable than the suggested shear-induced fragmentation within the oil [7] because the energies and forces involved are significantly

lower. Moreover, the reactive substrate allowed to isolate the organophosphorus units from the central Zn-S ones, thus explaining the evidence of separate phosphate and zinc sulfide areas observed experimentally [1,13].

Starting from the results obtained from bond stretching over a substrate (Fig. 6), we studied the energetics for subsequent molecular dissociations following two-, three- and four-fragments dissociation paths. This analysis is crucial to understand the adsorption energy cost/gain at the equilibrium for the different fragments forming within the tribofilm, helping the experimentalists to gain useful insight into stress-induced chemical reactions, which are almost impossible to detect during tribological experiments.

We performed a systematic study of fragments adsorption by employing Xsorb [46], a computational tool developed in our group, to perform a configurational study testing different fragment orientations for each system. For the substrates, we take into account the two opposite conditions of O-passivation, namely a bare Fe(110) surface and a complete oxygen-passivated (i.e., 1 ML) Fe(110) substrate. We found the optimal adsorption geometries reported in Fig. 7, together with the corresponding E_{frag}.

From the analysis shown in Fig. 7a, we found that the adsorption of the S-terminated (F1) and the organophosphorus fragments (F2) over the O-passivated substrate is highly endothermic, with an associated energy cost of + 2.54 eV. However, the same dissociation path on the bare iron substrate is energetically favourable, with E_{frag} equal to −4.39 eV. These results confirm the effectiveness of O-passivation in hindering the ZDDP fragmentation completely. We tested the further dissociation of F1 by considering a three-fragments dissociation path (Fig. 7b), which resulted in a further E_{frag} decrease to −5.71 eV. This result suggests that organophosphorus groups prefer to stay isolated
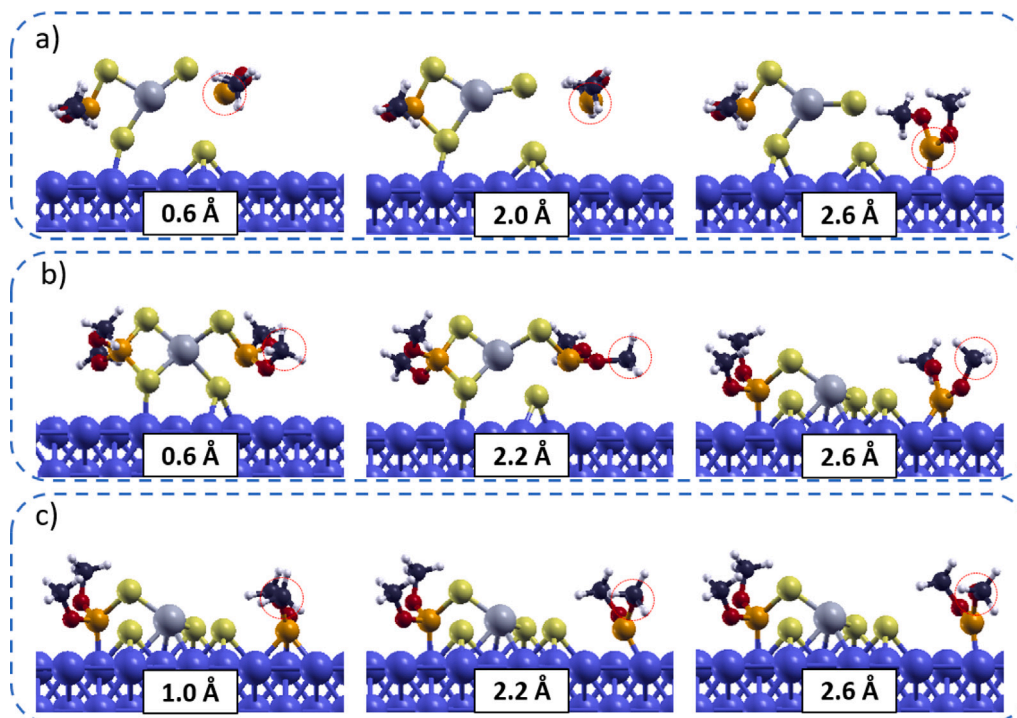
Fig. 6. ZDDP pulling on clean Fe. The atoms pulled, respectively P (panel a), C (panel b) and O (panel c) are highlighted with a dotted red circle. Atoms displacement is reported.
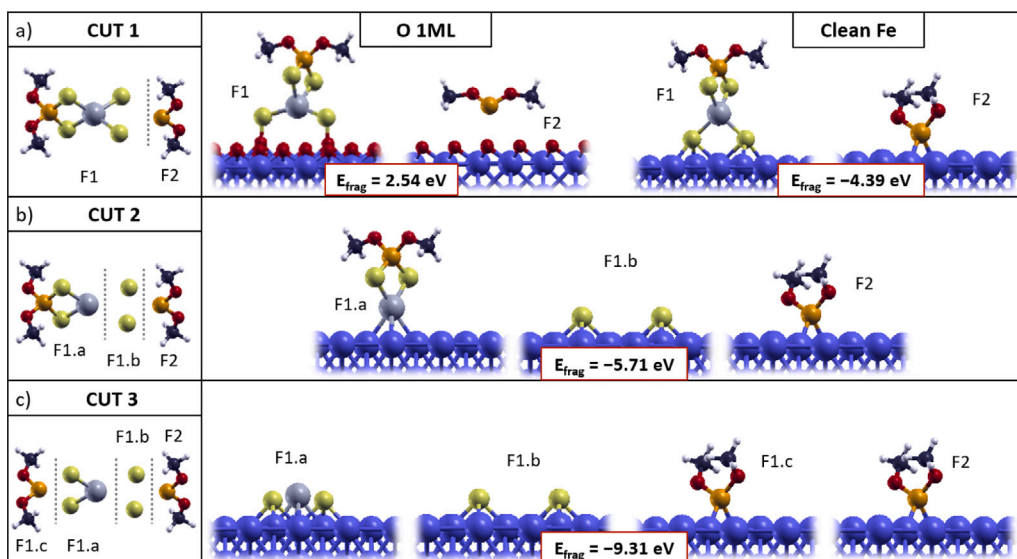

Fig. 7. ZDDP fragments adsorption following a two- (panel a), three- (panel b) and four-fragments (panel c) dissociation path. In panel (a) both adsorption on 1 ML O-passivated Fe and clean Fe are reported, while panel b and c involve bare iron only.

from the central units when adsorbed on iron, which is consistent with previous results of similar compounds on iron [51]. The complete fragmentation of the organophosphorus groups from the ZDDP (Fig. 7c) resulted in the lowest E_{frag} equal to −9.31 eV. Our findings shed light on the formation of zinc sulfide and phosphate layers commonly seen during tribological experiments [1,13]. We discovered that separating P-terminated groups from Zn-S central units is highly favourable. This insight may help tailor ZDDP stoichiometry to release only the specific groups needed for optimal tribofilm formation.

3.3. Load-induced ZDDP dissociation

To verify the effects of load on molecular dissociation, we performed uniaxial compressions of the molecule confined at an iron interface in the presence of 1 GPa load, as explained in the Methods section.

In Fig. 8, snapshots of the relaxation runs while reaching the target pressure are shown for the different oxidation levels. In Fig. 8a and b, the snapshots relative to the clean and 0.25 ML O-passivated iron substrates are shown. The same dissociative paths determined from equilibrium calculations at the open surface are displayed in both cases. In particular, both organophosphorus groups separate from the ZDDP molecule, leaving the Zn-S central units completely isolated. These insights gained by dissociative reactions are fascinating since no direct experimental evidence exists on the most favourable ZDDP fragmentation paths. For instance, organophosphorus units always need to be saturated due to the 5 valence electrons present in the P atom electronic configuration. Therefore, these fragments attracted the S atoms in the gas phase, breaking the Zn-S bonds. On the contrary,
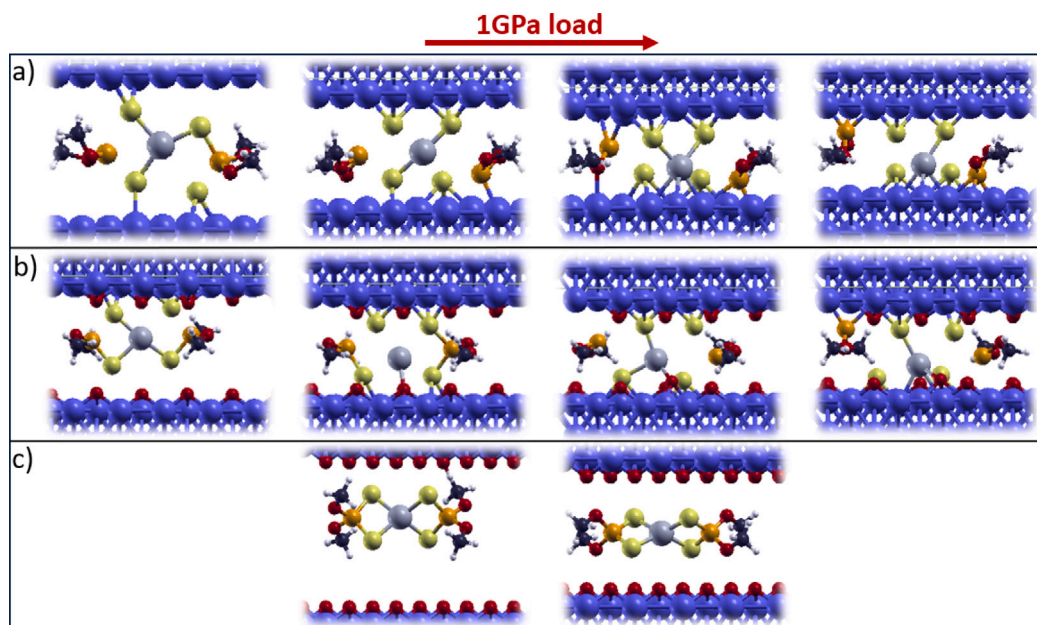
1GPa load

Fig. 8. Uniaxial compression optimizations for ZDDP on clean Fe (panel a), 0.25 ML O passivated Fe (panel b) and 1 ML O-passivated Fe (panel c). From left to right, different snapshots while reaching the target 1 GPa pressure are reported.

the reactive substrate helps stabilize the P-based groups that leave the molecule and adsorb on the surface.

Concerning the O-passivated iron surface at 1 ML, there are no dissociative reactions even when the external pressure is applied, and the ZDDP molecule only appears to be stretched. Therefore, the passivation of the iron substrate substantially reduces the molecular dissociation rate and impedes it at high O-coverages.

4. Conclusions

We employed DFT simulation to evaluate key processes involved in the early stages of ZDDP tribofilm formation, namely: molecular adsorption and its stress-induced fragmentation both in vacuum and on ferrous substrates with different oxidation levels.

- We have created a computational protocol to study the ZDDP dissociation pathway when mechanical stresses are applied. We displaced a specific atom along a certain direction, fixed its coordinate along the displacement direction and optimized the remainder of the molecule.
- We applied this protocol in two different scenarios: (i) ZDDP isolated in vacuum (representative of non-chemically reactive interactions) and (ii) adsorbed on a Fe(110) substrate.
- We found that the ZDDP dissociation process is highly endothermic in vacuum and energetically favourable over the substrate. Moreover, the reaction pathway also changes between the two scenarios. In particular, the iron substrate allows the detachment of organophosphorus groups from the central Zn-S units, in agreement with experimental evidence [11,14].
- We also observed the same reaction pathways over the substrate when a normal stress is applied rather than a tangential one. This evidence further strengthens our hypothesis that the organophosphorus groups and the central Zn-S serve as the building blocks for the zinc sulfide and phosphate layers detected in post-mortem analysis [1,13].
- Finally, we found that oxygen passivation and iron oxides (like hematite) significantly reduce the ZDDP molecular adsorption. Moreover, its dissociation is increasingly hampered when the oxygen concentration over the substrate is increased.

Overall, our results provide a first atomistic insight into ZDDP dissociation, which represents the first stage of film formation.

CRediT authorship contribution statement

Francesca Benini: Investigation, Writing – original draft. **Paolo Restuccia:** Investigation, Writing – review & editing. **M. Clelia Righi:** Conceptualization, Supervision, Funding acquisition, Writing – review & editing.

Declaration of competing interest

The authors declare that they have no known competing financial interests or personal relationships that could have appeared to influence the work reported in this paper.

Data availability

Data will be made available on request.

Acknowledgements

References

[1] H. Spikes, The history and mechanisms of ZDDP, Tribol. Lett. 17 (2004) 469–489, http://dx.doi.org/10.1023/B:TRIL.0000044495.26882.b5.

[2] A.M. Barnes, K.D. Bartle, V.R. Thibon, A review of zinc dialkyldithiophosphates (ZDDPS): characterisation and role in the lubricating oil, Tribol. Int. 34 (6) (2001) 389–395, http://dx.doi.org/10.1016/S0301-679X(01)00028-7.

[3] M.A. Nicholls, T. Do, P.R. Norton, M. Kasrai, G.M. Bancroft, Review of the lubrication of metallic surfaces by zinc dialkyl-dithiophosphates, Tribol. Int. 38 (1) (2005) 15–39, http://dx.doi.org/10.1016/j.triboint.2004.05.009.

[4] N. Gosvami, J. Bares, F. Mangolini, A. Konicek, D. Yablon, R. Carpick, Mechanisms of antiwear tribofilm growth revealed in situ by single-asperity sliding contacts, Science 348 (6230) (2015) 102–106, http://dx.doi.org/10.1126/science.1258788.

[5] A. Neville, A. Morina, T. Haque, M. Voong, Compatibility between tribological surfaces and lubricant additives—how friction and wear reduction can be controlled by surface/lube synergies, Tribol. Int. 40 (10–12) (2007) 1680–1695, http://dx.doi.org/10.1016/j.triboint.2007.01.019.

[6] J.M. Martin, Antiwear mechanisms of zinc dithiophosphate: a chemical hardness approach, Tribol. Lett. 6 (1999) 1–8, http://dx.doi.org/10.1023/A:1019191019134.

[7] J. Zhang, H. Spikes, On the mechanism of ZDDP antiwear film formation, Tribol. Lett. 63 (2016) 24, http://dx.doi.org/10.1007/s11249-016-0706-7.

[8] J. Zhang, J.P. Ewen, M. Ueda, J.S. Wong, H.A. Spikes, Mechanochemistry of zinc dialkyldithiophosphate on steel surfaces under elastohydrodynamic lubrication conditions, ACS Appl. Mater. Interfaces 12 (5) (2020) 6662–6676, http://dx.doi.org/10.1021/acsami.9b20059, URL: https://pubs.acs.org/doi/10.1021/acsami.9b20059.

[9] P. Parsaeian, A. Ghanbarzadeh, M.C. Van Eijk, I. Nedelcu, A. Neville, A. Morina, A new insight into the interfacial mechanisms of the tribofilm formed by zinc dialkyl dithiophosphate, Appl. Surf. Sci. 403 (2017) 472–486, http://dx.doi.org/10.1016/j.apsusc.2017.01.178, URL: https://www.sciencedirect.com/science/article/pii/S0169433217302003.

[10] K. Topolovec-Miklozic, T.R. Forbus, H.A. Spikes, Film thickness and roughness of ZDDP antiwear films, Tribol. Lett. 26 (2007) 161–171, http://dx.doi.org/10.1007/s11249-006-9189-2, URL: https://link.springer.com/article/10.1007/s11249-006-9189-2.

[11] M. Ueda, A. Kadiric, H. Spikes, On the crystallinity and durability of ZDDP tribofilm, Tribol. Lett. 67 (2019) 1–13, http://dx.doi.org/10.1007/s11249-019-1236-x, URL: https://link.springer.com/article/10.1007/s11249-019-1236-x.

[12] L. Fang, S. Korres, W.A. Lamberti, M.N. Webster, R.W. Carpick, What stress components drive mechanochemistry? A study of ZDDP tribofilm formation, Faraday Discuss. 241 (2023) 394–412, http://dx.doi.org/10.1039/D2FD00123C.

[13] A. Dorgham, A. Azam, A. Morina, A. Neville, On the transient decomposition and reaction kinetics of zinc dialkyldithiophosphate, ACS Appl. Mater. Interfaces 10 (51) (2018) 44803–44814, http://dx.doi.org/10.1021/acsami.8b08293, URL: https://pubs.acs.org/doi/10.1021/acsami.8b08293.

[14] R. Heuberger, A. Rossi, N.D. Spencer, XPS study of the influence of temperature on ZnDTP tribofilm composition, Tribol. Lett. 25 (2007) 185–196, http://dx.doi.org/10.1007/s11249-006-9166-9, URL: https://link.springer.com/article/10.1007/s11249-006-9166-9.

[15] S.V. Sukhomlinov, M.H. Müser, Stress anisotropy severely affects zinc phosphate network formation, Tribol. Lett. 69 (2021) 89, http://dx.doi.org/10.1007/s11249-021-01462-6.

[16] D. Kumar, J. Jain, N.N. Gosvami, In situ study of role of microstructure on antiwear tribofilm formation on AZ91 magnesium alloy under zinc dialkyldithiophosphate containing lubricant, Adv. Eng. Mater. 22 (2020) 2000335, http://dx.doi.org/10.1002/adem.202000335.

[17] N.J. Mosey, M.H. Muser, T.K. Woo, Molecular mechanisms for the functionality of lubricant additives, Science 307 (5715) (2005) 1612–1615, http://dx.doi.org/10.1126/science.1107895.

[18] Y. Chen, P. Renner, H. Liang, A review of current understanding in tribochemical reactions involving lubricant additives, Friction 11 (2022) 1–24, http://dx.doi.org/10.1007/s40544-022-0637-2.

[19] S. Peeters, P. Restuccia, S. Loehlé, B. Thiebaut, M.C. Righi, Tribochemical reactions of MoDTC lubricant additives with iron by Quantum Mechanics/Molecular Mechanics simulations, J. Phys. Chem. C 124 (2020) 13688–13694, http://dx.doi.org/10.1021/acs.jpcc.0c02211.

[20] H. Spikes, Stress-augmented thermal activation: Tribology feels the force, Friction 6 (2018) 1–31, http://dx.doi.org/10.1007/s40544-018-0201-2, URL: https://link.springer.com/article/10.1007/s40544-018-0201-2.

[21] M. Suominen Fuller, K. De Jong, M. Kasrai, G. Bancroft, Electroless generation of phosphate films on metals from zinc dialkyldithiophosphates, Chem. Mater. 12 (5) (2000) 1300–1304, http://dx.doi.org/10.1021/cm990636t.

[22] M. Mee, A. Torrance, A study of the lubricated wear of plain bearing materials in a ZDDP-containing lubricant, Wear 128 (2) (1988) 201–217, http://dx.doi.org/10.1016/0043-1648(88)90185-8.

[23] J. Sheasby, T. Caughlin, W. Mackwood, A comparison of the boundary lubrication of 52100 steel, zirconia and silicon nitride by S, P, S/P and zinc dialkyl dithiophosphate additives, Wear 196 (1–2) (1996) 100–109, http://dx.doi.org/10.1016/0043-1648(95)06862-7.

[24] B. Mingwu, Z. Xushou, Q. Shangkui, Tribological properties of silicon nitride ceramics coated with molybdenum films under boundary lubrication, Wear 169 (2) (1993) 181–187, http://dx.doi.org/10.1016/0043-1648(93)90296-X.

[25] T. Haque, A. Morina, A. Neville, R. Kapadia, S. Arrowsmith, Non-ferrous coating/lubricant interactions in tribological contacts: assessment of tribofilms, Tribol. Int. 40 (10–12) (2007) 1603–1612, http://dx.doi.org/10.1016/j.triboint.2007.01.023.

[26] T. Haque, A. Morina, A. Neville, R. Kapadia, S. Arrowsmith, Study of the ZDDP antiwear tribofilm formed on the DLC coating using AFM and XPS techniques, 1501 STP, ASTM International, 2008, pp. 92–102, http://dx.doi.org/10.1520/stp45586s,

[27] G. Losi, S. Peeters, F. Delayens, H. Vezin, S. Loehlé, B. Thiebaut, M.C. Righi, Experimental and Ab initio characterization of mononuclear molybdenum dithiocarbamates in lubricant mixtures, Langmuir 37 (16) (2021) 4836–4846, http://dx.doi.org/10.1021/acs.langmuir.1c00029.

[28] S. Peeters, C. Charrin, I. Duron, S. Loehlé, B. Thiebaut, M.C. Righi, Importance of the catalytic effect of the substrate in the functionality of lubricant additives: the case of molybdenum dithiocarbamates, Mater. Today Chem. 21 (2021) 100487, http://dx.doi.org/10.1016/J.MTCHEM.2021.100487.

[29] X. Liu, L. Sun, W.-Q. Deng, Theoretical investigation of CO2 adsorption and dissociation on low index surfaces of transition metals, J. Phys. Chem. C 122 (15) (2018) 8306–8314, http://dx.doi.org/10.1021/acs.jpcc.7b12660.

[30] M. Vanzan, M. Marsili, S. Corni, Study of the rate-determining step of Rh catalyzed CO2 reduction: Insight on the hydrogen assisted molecular dissociation, Catalysts 11 (5) (2021) http://dx.doi.org/10.3390/catal11050538, URL: https://www.mdpi.com/2073-4344/11/5/538.

[31] C. Ayestarán Latorre, J.E. Remias, J.D. Moore, H.A. Spikes, D. Dini, J.P. Ewen, Mechanochemistry of phosphate esters confined between sliding iron surfaces, Commun. Chem. 4 (1) (2021) 178, http://dx.doi.org/10.5281/zenodo.5708426, URL: https://www.nature.com/articles/s42004-021-00615-x.

[32] N.J. Mosey, T.K. Woo, Finite temperature structure and dynamics of zinc dialkyldithiophosphate wear inhibitors: A density functional theory and ab initio molecular dynamics study, J. Phys. Chem. A 107 (2003) 5058–5070, http://dx.doi.org/10.1021/jp034085c.

[33] S.V. Sukhomlinov, G. Kickelbick, M.H. Müser, Mechanochemical ionization: Differentiating pressure-, shear-, and temperature-induced reactions in a model phosphate, Tribol. Lett. 70 (2022) 102, http://dx.doi.org/10.1007/s11249-022-01644-w.

[34] N.J. Mosey, T.K. Woo, A quantum chemical study of the unimolecular decomposition mechanisms of zinc dialkyldithiophosphate antiwear additives, J. Phys. Chem. A 108 (28) (2004) 6001–6016, http://dx.doi.org/10.1021/jp049371i, URL: https://pubs.acs.org/doi/10.1021/jp049371i.

[35] P. Giannozzi, S. Baroni, N. Bonini, M. Calandra, R. Car, C. Cavazzoni, D. Ceresoli, G.L. Chiarotti, M. Cococcioni, I. Dabo, et al., QUANTUM ESPRESSO: a modular and open-source software project for quantum simulations of materials, J. Phys.: Condens. Matter 21 (2009) 395502, http://dx.doi.org/10.1088/0953-8984/21/39/395502.

[36] P. Giannozzi, O. Andreussi, T. Brumme, O. Bunau, M.B. Nardelli, M. Calandra, R. Car, C. Cavazzoni, D. Ceresoli, M. Cococcioni, et al., Advanced capabilities for materials modelling with Quantum ESPRESSO, J. Phys.: Condens. Matter 29 (2017) 465901, http://dx.doi.org/10.1088/1361-648X/aa8f79.

[37] P. Giannozzi, O. Baseggio, P. Bonfà, D. Brunato, R. Car, I. Carnimeo, C. Cavazzoni, S.D. Gironcoli, P. Delugas, F.F. Ruffino, et al., Quantum ESPRESSO toward the exascale, J. Chem. Phys. 152 (2020) 154105, http://dx.doi.org/10.1063/5.0005082.

[38] J.P. Perdew, K. Burke, M. Ernzerhof, Generalized gradient approximation made simple, Phys. Rev. Lett. 77 (1996) 3865, http://dx.doi.org/10.1103/PhysRevLett.77.3865.

[39] V.I. Anisimov, J. Zaanen, O.K. Andersen, Band theory and mott insulators: Hubbard U instead of stoner I, Phys. Rev. B 44 (3) (1991) 943, http://dx.doi.org/10.1103/PhysRevB.44.943, URL: https://journals.aps.org/prb/abstract/10.1103/PhysRevB.44.943.

[40] M.-T. Nguyen, N. Seriani, R. Gebauer, Water adsorption and dissociation on α-Fe2O3 (0001): PBE+ U calculations, J. Chem. Phys. 138 (19) (2013) http://dx.doi.org/10.1063/1.4804999, URL: https://pubs.aip.org/aip/jcp/article-abstract/138/19/194709/192327/Water-adsorption-and-dissociation-on-Fe2O3-0001?redirectedFrom=fulltext.

[41] R.B. Wang, A. Hellman, Initial water adsorption on hematite (α-Fe2O3)(0001): A DFT+ U study, J. Chem. Phys. 148 (9) (2018) http://dx.doi.org/10.1063/1.5020358, URL: https://pubs.aip.org/aip/jcp/article-abstract/148/9/094705/196817/Initial-water-adsorption-on-hematite-Fe2O3-0001-A?redirectedFrom=fulltext.

[42] N.Y. Dzade, A. Roldan, N.H. De Leeuw, A density functional theory study of the adsorption of benzene on hematite (α-fe2o3) surfaces, Minerals 4 (1) (2014) 89–115, http://dx.doi.org/10.3390/min4010089, URL: https://www.mdpi.com/2075-163X/4/1/89.

[43] A.M. Rappe, K.M. Rabe, E. Kaxiras, J.D. Joannopoulos, Optimized pseudopotentials, Phys. Rev. B 41 (1990) 1227–1230, http://dx.doi.org/10.1103/PhysRevB.41.1227, URL: https://link.aps.org/doi/10.1103/PhysRevB.41.1227.

[44] S. Peeters, A. Barlini, J. Jain, N.N. Gosvami, M.C. Righi, Adsorption and decomposition of ZDDP on lightweight metallic substrates: Ab initio and experimental insights, Appl. Surf. Sci. 600 (2022) 153947, http://dx.doi.org/10.1016/J.APSUSC.2022.153947.

[45] H.T.T. Ta, N.V. Tran, M.C. Righi, Atomistic wear mechanisms in diamond: Effects of surface orientation, stress, and interaction with adsorbed molecules, 2023, http://dx.doi.org/10.1021/acs.langmuir.3c01800, URL: https://pubs.acs.org/doi/10.1021/acs.langmuir.3c01800 accepted for publication in Langmuir.

[46] E. Pedretti, P. Restuccia, M.C. Righi, Xsorb: a software for identifying the most stable adsorption configuration and energy of a molecule on a crystal surface, Comput. Phys. Comm. 291 (2023) 108827, http://dx.doi.org/10.1016/j.cpc.2023.108827, URL: https://www.sciencedirect.com/science/article/pii/S0010465523001728.

[47] S. Peeters, P. Restuccia, S. Loehlé, B. Thiebaut, M. Righi, Characterization of molybdenum dithiocarbamates by first-principles calculations, J. Phys. Chem. A 123 (32) (2019) 7007–7015, http://dx.doi.org/10.1021/acs.jpca.9b03930.

[48] B. Dacre, C. Bovington, The adsorption and desorption of zinc di-isopropyldithiophosphate on steel, ASLE Trans. 25 (4) (1982) 546–554, http://dx.doi.org/10.1080/05698198208983124.

[49] N. Gosvami, I. Lahouij, J. Ma, R. Carpick, Nanoscale in situ study of ZDDP tribofilm growth at aluminum-based interfaces using atomic force microscopy, Tribol. Int. 143 (2020) 106075, http://dx.doi.org/10.1016/j.triboint.2019.106075, URL: https://www.sciencedirect.com/science/article/pii/S0301679X19305894.

[50] W. Tuszynski, J. Molenda, M. Makowska, Tribochemical conversions of zinc dialkyldithiophosphate (ZDDP) under extremely different pressure conditions, Tribol. Lett. 13 (2) (2002) 103–109, http://dx.doi.org/10.1023/A:1020104732624, URL: https://link.springer.com/article/10.1023/A:1020104732624.

[51] M.C. Righi, S. Loehlé, M.I. de Barros Bouchet, D. Philippon, J.M. Martin, Trimethyl-phosphite dissociative adsorption on iron by combined first-principle calculations and XPS experiments, RSC Adv. 5 (2015) 101162–101168, http://dx.doi.org/10.1039/C5RA14446A.